PIER C

(Received 16 November 2023, Accepted 4 January 2024, Scheduled 21 January 2024)

A Flexible UWB Slot Antenna with Quad Band-Notched Characteristics for Wearable Application

Tian-Shi Wang, Cheng-Zhu Du*, Hai-Feng Shu, and Zhi-Hua Yue

College of Electronics and Information Engineering, Shanghai University of Electric Power, Shanghai 200090, China

ABSTRACT: The design and analysis of a compact coplanar waveguide (CPW) fed wearable slot antenna with four notched bands for ultra-wideband (UWB) applications are presented in this paper. The antenna is printed on a 0.1-millimeter-thick liquid crystal polymer (LCP) substrate, providing flexibility for wearable applications. Split concentric rings (SCRs) engraved on the radiating patch and L-shaped branches loaded on the ground plane provide the antenna's notched features. The impedance bandwidth of the measured antenna ranges from 2.46 GHz to 12.52 GHz, with a fractional bandwidth (FBW) of 134.1%, and it exhibits notched bands covering specific frequency ranges, ranging from 2.84 GHz to 3.93 GHz for WiMAX applications, 4.84 GHz to 5.41 GHz for WLAN downlink, 5.66 GHz to 6.26 GHz for WLAN uplink, and 6.94 GHz to 7.79 GHz for X-band satellite communication. Furthermore, the gain of the proposed antenna varies between 1.5 and 6 dBi, excluding the notched band. The antenna is tested, and the flexibility performance is good. In a word, the fabricated antenna shows promising prospects for wearable applications.

1. INTRODUCTION

In recent years, there has been a notable surge in interest towards ultra-wideband (UWB) technology, driven by the increasing need for high-speed wireless communication systems. This technology offers numerous advantages, including remarkable data transfer speeds, efficient power utilization, and robust resistance to interference [1]. However, the design of a UWB antenna that consistently delivers predictable performance across the entire frequency band presents a formidable challenge. Such an antenna must not only exhibit high radiation efficiency, but also accommodate the wide UWB bandwidth. Recently, UWB antennas with bands rejection characteristics have been proposed, which can prevent interference with other narrowband services, such as telemetry/mobile communications, WLAN and ITU bands [2–13]. Wearable UWB technology has garnered significant attention for its transformative potential in communication [14–16], health monitoring, and medical applications [17]. With this rising interest in wearables, flexible UWB antennas have become a focal point of research and development.

Several UWB antennas featuring multiple notched bands have been designed. An antenna with a circular monopole design for UWB applications is presented in [8], and the antenna discards two frequency bands of 5–5.6 GHz and 7.3–8.3 GHz. In [9], a UWB antenna with three notch bands of 1.8–2.3 GHz, 3.2–3.8 GHz, and 5.6–6.1 GHz is presented. The antenna is printed on an FR-4 substrate. In [10], by etching split concentric rings (SCR) on the patch, an antenna achieves four bands rejection characteristics. In [11], introducing a flexible, wearable UWB antenna with WLAN applications and distinctive notch characteristics is presented. The substrate of the antenna is made of denim (jeans fabric). In [12], a flexible elliptical antenna for wireless communications is presented. The UWB antenna has notch characteristics at 2–2.7 GHz, 3.45–3.8 GHz, and 5.15–6.2 GHz.

In this article, a wearable UWB slot antenna built on a flexible substrate is proposed. Based on an ultrathin liquid crystal polymer (LCP) substrate, the antenna exhibits excellent stability across a wide range of temperatures and in humid environments. The antenna has notch characteristics at 3.1–4.0 GHz, 4.7–5.5 GHz, 5.7–6.2 GHz, and 7.0–7.8 GHz, rejecting WiMAX, WLAN, and X-band satellite communication. The antenna was measured in free space, bent environments, and close to the human body. Investigations were conducted on the antenna's radiation traits and specific absorption rate (SAR) values.

The innovation points of the proposed antenna include: (1) Four notch bands are formed at the flexible antenna. (2) The antenna is compact and flexible, making it suitable for wearable application. (3) Using CPW feeding, it has low loss, low dispersion, and is easier to integrate with microwave circuits.

2. DESIGN AND ANALYSIS OF THE ANTENNA

2.1. Design Process of the Ultra-Wideband (UWB) Antenna

This ultra-wideband antenna has dimensions of 30 mm × 30 mm × 0.1 mm. It is printed on a LCP substrate. The dielectric constant of LCP is 2.9, and the loss tangent is 0.02. Figure 1 depicts the UWB antenna's design process. Initially, the antenna is designed as a slotted antenna (Antenna #1) using a compact coplanar waveguide (CPW) feeding technique. The radius of the circular patch is calculated

* Corresponding author: Chengzhu Du (duchengzhu@163.com).

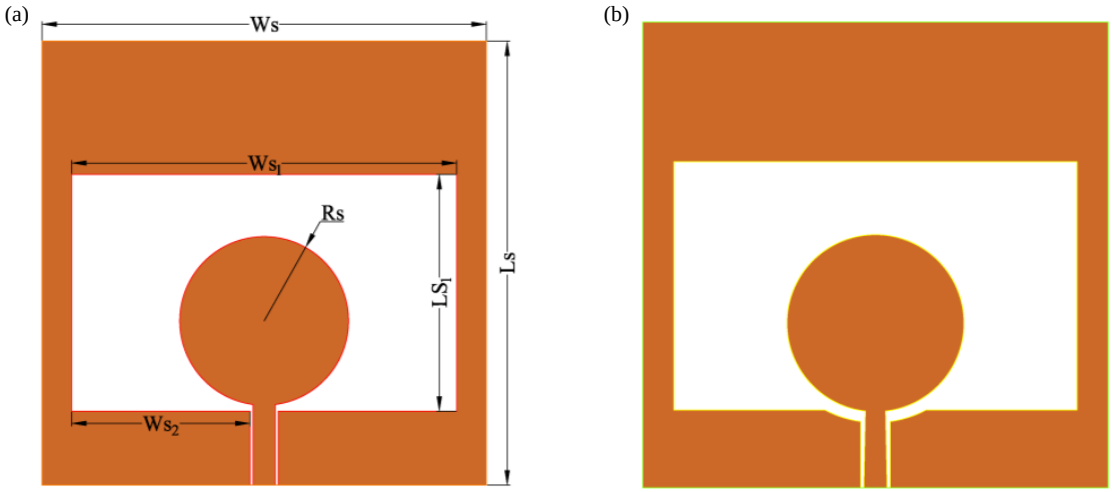

FIGURE 1. Evolution steps of the UWB antenna, (a) Antenna #1, (b) Antenna #2.

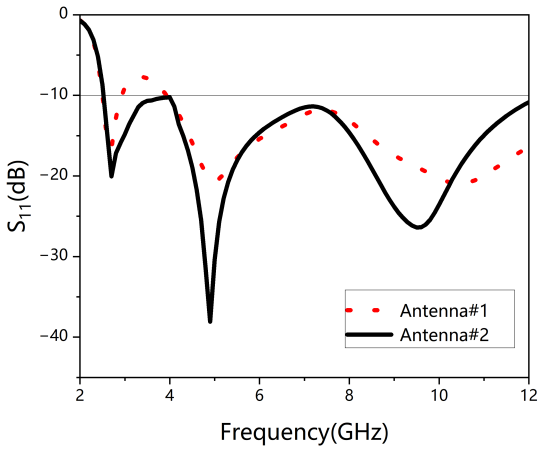

FIGURE 2. Simulated return loss characteristics of various antennas.

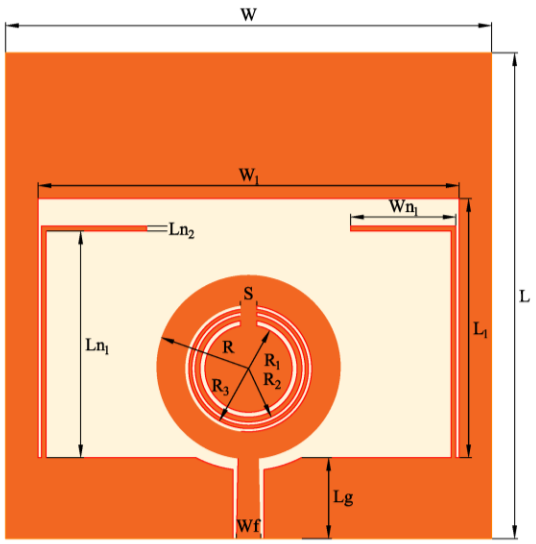

FIGURE 3. The geometry of the quad band-notched UWB antenna.

using the formula [10]:

$$R = \frac{F}{\sqrt{1 + \frac{2h}{\pi\varepsilon_{eff}F\left[\ln\left(\frac{F\pi}{2h}\right)+1.7726\right]}}}, \quad F = \frac{8.791 \times 10^9}{f_c\sqrt{\varepsilon_{eff}}}, \quad (1)$$

where R is the radius of the circular patch, ε_{eff} the dielectric constant of substrate, h the height of substrate, and $f_c = 5$ GHz is the resonant frequency.

The antenna size parameters of the UWB slot antenna after optimization using Ansys HFSS are as follows: $Ws = 30$ mm, $Ls = 30$ mm, $Ls_1 = 16$ mm, $Ws_1 = 26$ mm, $Ws_2 = 12$ mm, $Rs = 5.7$ mm.

It has two symmetrical ground planes and a round radiator positioned on the substrate's front side. To further extend the impedance bandwidth, the dimensions of the feedline for Antenna #2 are gradually modified. To produce a defected ground structure, slots are added to the symmetrical ground plane. Figure 2 displays the return loss characteristics of Antenna #1 and Antenna #2. The bandwidth of Antenna #2 ranges from 2.53 GHz to 12 GHz.

2.2. Methods for Acquiring Notch Band Properties

Figure 3 shows the structure of an ultra-wideband slot antenna with four notch bands. Based on the previously designed UWB antenna, the antenna achieves four frequency band suppressions within the UWB frequency range by adding two symmetrical L-shaped branches to the ground planes and engraving three split concentric rings (SCRs) on the circular radiator. Figure 4 displays a step-by-step presentation of the antenna, illustrating the evolution of each notch band and its corresponding S_{11} value. In step 1, the L-shaped branches on the ground plane are employed to suppress the notch band from 2.84 GHz

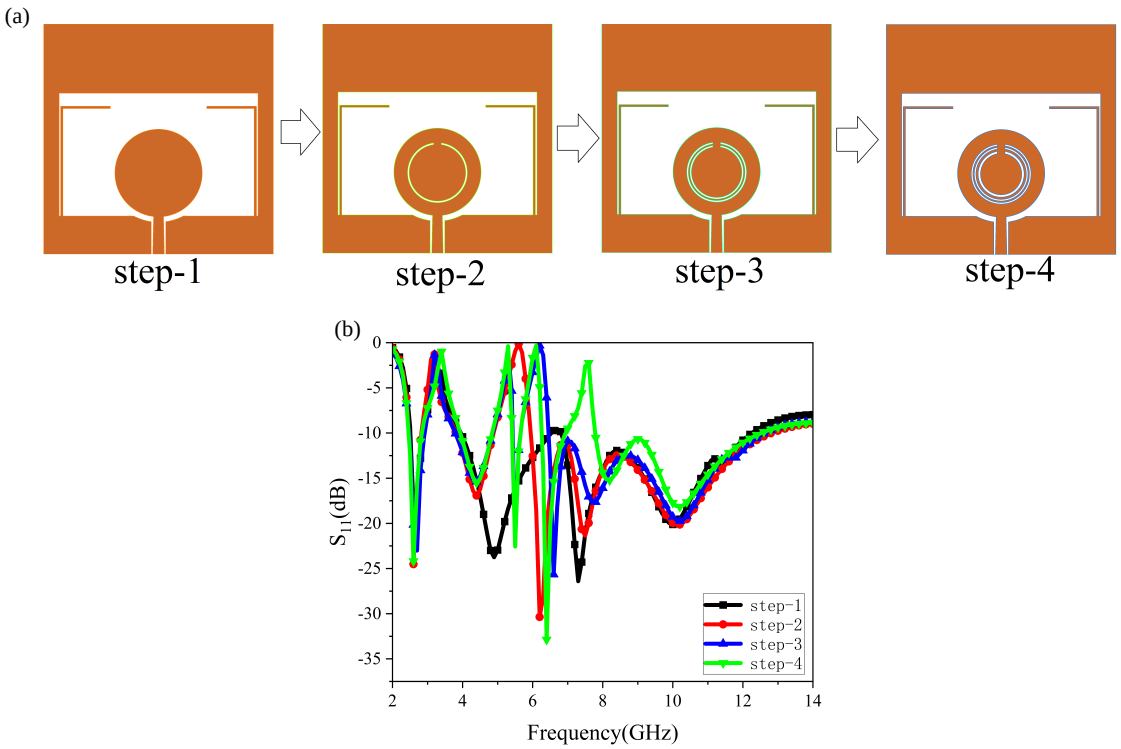

FIGURE 4. (a) Step-wise evolution of the antenna with band-notched characteristics. (b) S_{11} of the step-wise evolution of the antenna.

to 3.93 GHz. In step 2, the first SCR is added to get the notch band from 4.84 GHz to 5.41 GHz. In step 3, the second SCR is added to get the notch band from 5.66 GHz to 6.26 GHz. In step 4, the third SCR is added to get the notch band from 6.94 GHz to 7.79 GHz. The entire bandwidth of the antenna ranges from 2.46 GHz to 12.52 GHz, with dimensional parameters listed in Table 1. The lengths of the L-shaped branches and SCR are usually $\frac{\lambda}{4}$ determined by the following formula:

$$L = \frac{C}{4f_c \cdot \sqrt{\varepsilon_{eff}}} \tag{2}$$

where C is the velocity of light, f_c the center frequency of the notch band, and ε_{eff} the effective dielectric constant.

TABLE 1. Optimized design parameters of the antenna. (Unit: mm).

W	W_1	Wn_1	Wf	L	L_1	Ln_1
30	26	6.5	1.5	30	7	12
Ln_2	Lg	R	R_1	R_2	R_3	S
0.2	5	5.7	2.7	3.3	3.7	1

2.3. Parameter Analysis

Figure 5 shows the impact of adjusting the dimensions of the L-shaped branches and SCRs on the the antenna. The key parameter of the L-shaped branches is denoted as Ln_1, and the key parameters of the three SCRs elements are denoted as R_3, R_2, and R_1. The centre frequency of the first notched band is mostly influenced by the parameter Ln_1. The centre frequencies of the three notch bands are mostly influenced by the parameters R_3, R_2, and R_1, respectively. On the other hand, the four notch bands have little influence on each other.

3. RESULTS AND DISCUSSION

3.1. Simulated and Measured S-Parameter

Figure 6(a) displays the antenna's real processing diagram. The performances of the proposed antenna were simulated at Ansys HFSS software, and the results are clearly displayed in Figure 6(b), which shows the reflection loss ($|S_{11}|$) of the UWB antenna with four notched characteristics. The measured operating bandwidth range, where $S_{11} < -10$ dB, extends from 2.7 GHz to 10 GHz. The measured notched frequencies of the antenna are located at 3.1–4 GHz, 4.7–5.5 GHz, 5.7–6.2 GHz, and 7–7.8 GHz, effectively suppressing interference signals such as WiMAX (3.3–3.7 GHz), WLAN downlink (5.15–5.35 GHz), WLAN uplink (5.725–5.825 GHz), and X-band satellite communication (7.25–7.75 GHz). Each notched band exhibits a peak value greater than -5 dB, presenting the good band-rejection properties of the antenna. The measured S_{11} is almost identical to the simulated S_{11}, with certain variations ascribed to flaws in the manufacturing process, as well as the surroundings and the antenna testing apparatus's inability to provide optimal testing conditions, such as cables.

3.2. The Current Distribution

The distributions of current at four notched frequencies (3.4 GHz, 5.2 GHz, 6.1 GHz, 7.6 GHz) are displayed in Figure 7. Observations reveal that at 3.4 GHz, the current primarily distributes on the two symmetrical L-shaped branches

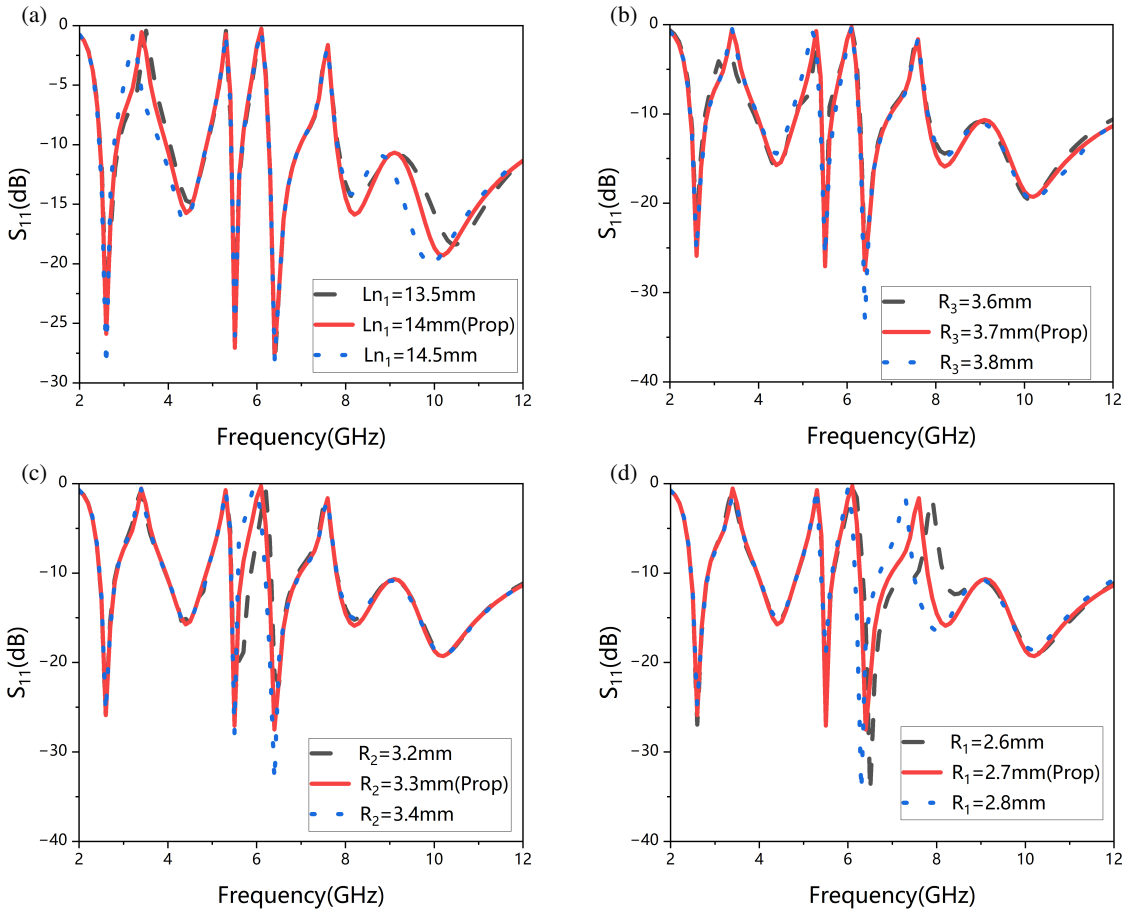

FIGURE 5. Simulated S_{11} plot for variation in (a) Ln_1, (b) R_3, (c) R_2, (d) R_1.

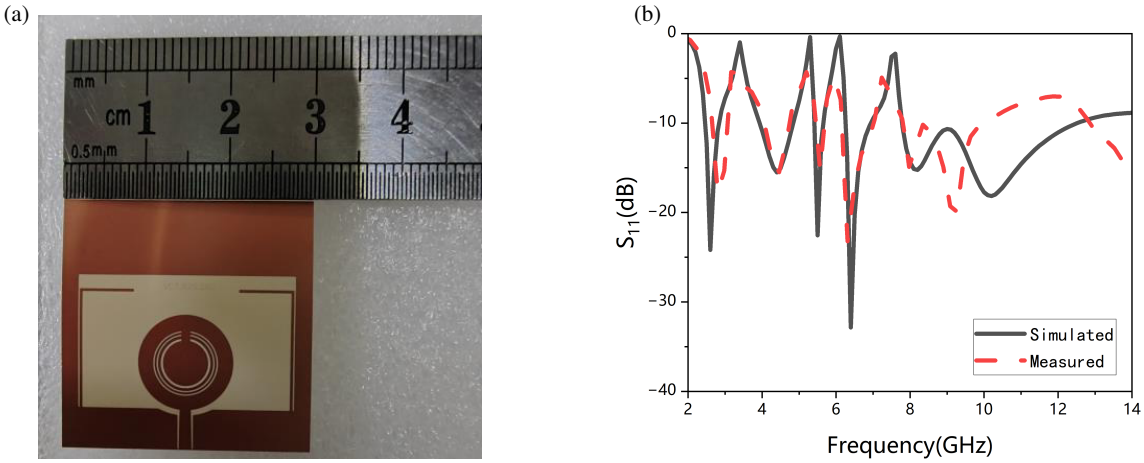

FIGURE 6. (a) Fabricated antenna prototype. (b) Simulated and measured S-parameters of the antenna.

on the ground plane. At 5.2 GHz, the current primarily resides above the outermost SCR notch. At 6.1 GHz, the current mainly resides above the central SCR notch, and at 7.6 GHz, the current mainly resides above the innermost SCR notch. Moreover, these locations of maximum currents are symmetrical along the H-plane, and the currents flow in opposite directions, which effectively cancel out the radiation fields and create the notched bands.

3.3. Radiation Patterns and Gain Analysis

Figure 8 illustrates the radiation pattern's measured and simulated outcomes at two representative non-notch band frequency points, 2.6 GHz and 6.4 GHz. It is evident that at 2.6 GHz and 6.4 GHz, the antenna exhibits an "8" shape radiation pattern in the E-plane and omnidirectional radiation in the H-plane, indicating that the antenna is suitable for receiving and transmitting signals from any direction in the working frequency band.

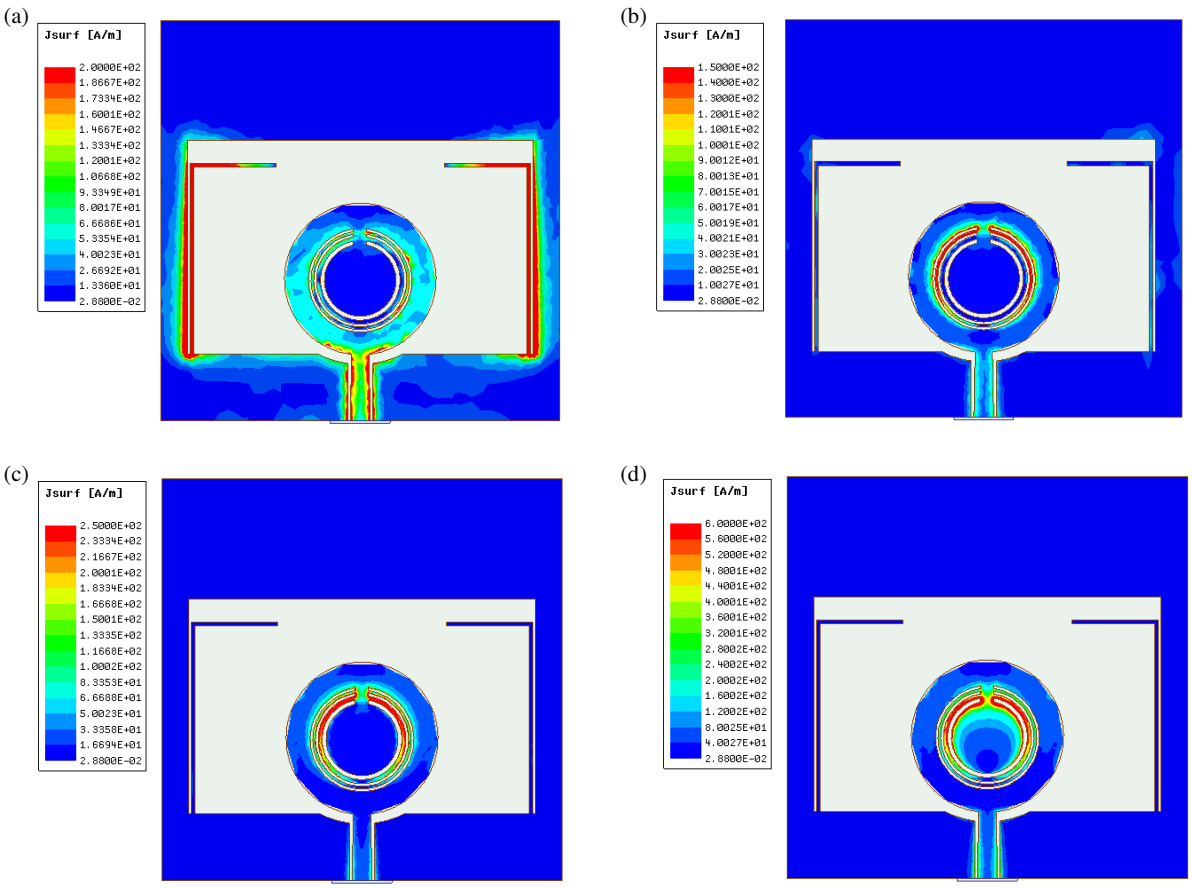

FIGURE 7. Surface current plot on the patch and ground plane at (a) 3.4 GHz, (b) 5.2 GHz, (c) 6.1 GHz, (d) 7.6 GHz.

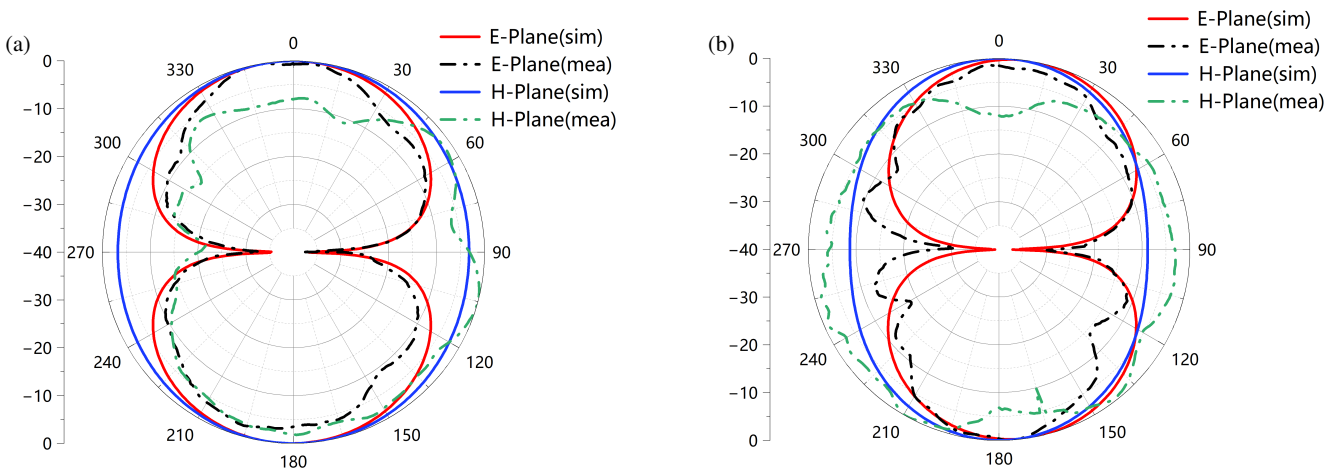

FIGURE 8. The simulated and measured E-plane and H-plane radiation patterns at (a) 2.4 GHz; (b) 6.4 GHz.

In addition, the simulated and measured realized gains of the antenna are given in Figure 9. The peak gain of the antenna sharply decreases at the notch band frequencies, and most of the notch bands achieve negative gain values, reflecting the excellent band-notched characteristics of the antenna. In other working frequency bands, the maximum gain of the antenna exceeds 6 dB, proving that the antenna's radiation properties in the operational frequency region are adequate.

3.4. Flexibility Study

We examined the antenna's S_{11} values when it was bent along the H-plane in order to assess its flexibility. The thickness of the LCP substrate utilized for the antenna is only 0.1 millimeters. In experiment measurement, we securely mounted the antenna on cylinders with radii of 30 and 50 millimeters, respectively. The bent S_{11} curves are plotted under different curvature

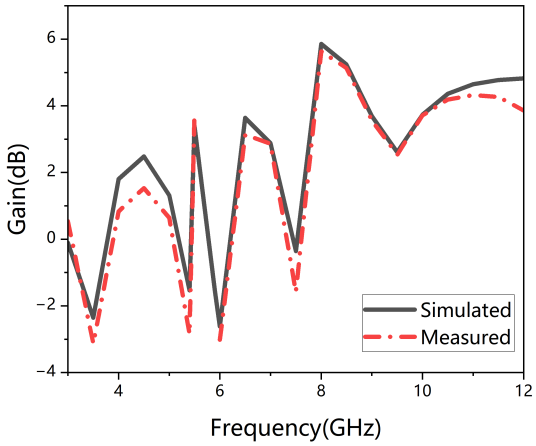

FIGURE 9. The simulated and measured peak gain.

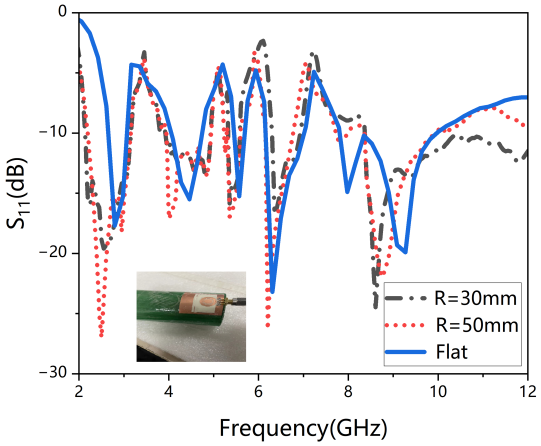

FIGURE 10. The measured S_{11} of the antenna when flat and bend.

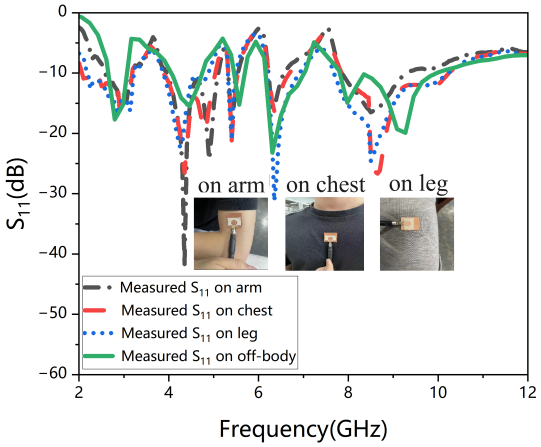

FIGURE 11. The measured S_{11} of the antenna placed on human body.

TABLE 2. Performance comparison with previous antennas.

Ref.	Sub	Flexibility	Bandwidth (GHz)	Size (mm)	No. of notches	Peak gain	Feeder method
[6]	FR4	No	2.5–12	37 × 46	2	4	Microstrip feed
[8]	FR4	No	3.7–13.3	19 × 13	2	4	Microstrip feed
[9]	FR4	No	1.4–11.3	33 × 34	3	4.6	Microstrip feed
[10]	RT/DUROID	No	3–11.6	30 × 23	4	5.11	CPW feed
[11]	Jeans	Yes	2.4–11.25	23 × 38	2	4.8	Microstrip feed
[12]	Teflon	Yes	1.05–13	45 × 35	3	5.4	CPW feed
Prop	LCP	Yes	2.7–10	30 × 30	4	6	CPW feed

radii, as shown in Figure 10. It can be found that under bending conditions, there is a slight shift in the frequencies of the notch bands, and the impedance bandwidth ($S_{11} < -10$ dB) of the bending antenna shows slight changes compared to flat antenna, but still meets the design requirements.

3.5. The Effects of the Human Body

The antenna, which utilizes flexible materials, is suitable for applications in the wearable field. To investigate the performances of the antenna close to the human body, we measured the antenna on the arm, chest, and leg. Figure 11 shows the antenna's measured S-parameter measurements at various body regions. When an antenna is positioned on a human body, observations have shown that its bandwidth experiences a significant reduction, and the position of the notch bands slightly shifts. Specifically, the first and second notch bands become narrower, with the third and fourth notch bands widened.

3.6. Specific Absorption Rate Evaluation

In wearable antenna applications, the impact of antenna radiation energy on human tissues is often quantitatively measured using specific absorption rate (SAR). In the simulation, the hu-

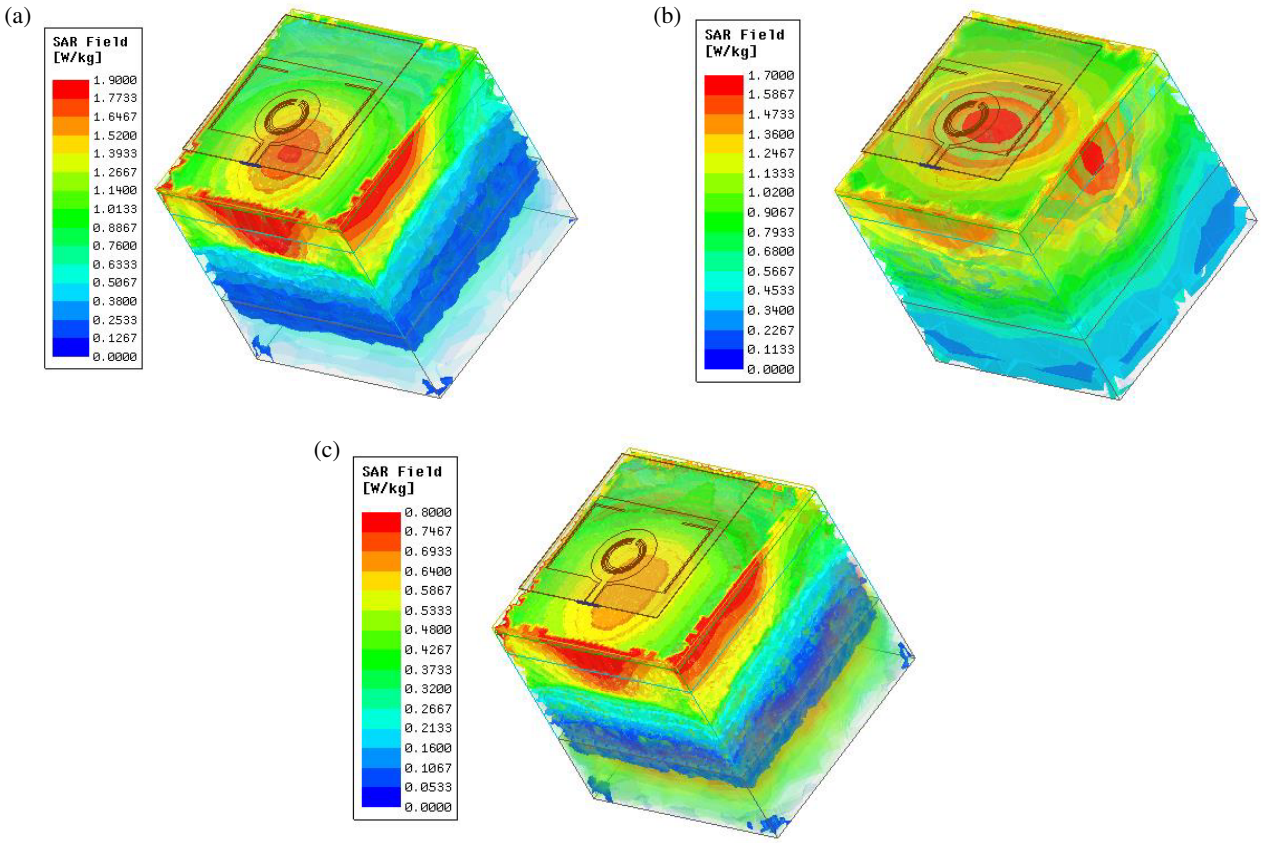

FIGURE 12. The SAR dispersion of the antenna closed to human tissue at (a) 2.4 GHz; (b) 6.4 GHz; (c) 9 GHz.

man body model is represented by four layers: skin, fat, muscle, and bone. Each layer has a specific thickness: 1 mm for the skin, 5 mm for the fat, 20 mm for the muscle, and 14 mm for the bone. Overall, the human body model has a total thickness of 40 mm. The separation between the antenna and the model of human tissue is 5 mm, and the input power is 0.1 watt. We simulated the SAR values in 10 g of biological tissue at 2.4 GHz, 6.4 GHz, and 9 GHz. Figure 12 displays the three-dimensional distribution of SAR of the antenna. It indicates that the SAR values for each 10 grams of tissue contain less than 2 W/kg, which meets the European standard for radiation exposure.

3.7. Performance Comparison

Compared with antennas presented in [6, 8–10], the proposed antenna utilizes a flexible LCP substrate, instead of a rigid dielectric substrate. Compared with the flexible antennas with notch bands proposed in [11, 12], the presented flexible antenna has more notch bands than others. Table 2 shows that the presented flexible antenna has smaller dimensions, more notch bands, and higher gain. Importantly, the antenna can be applied in the field of wearable devices.

4. CONCLUSION

A flexible CPW feed UWB slot antenna with quadruple band-notched characteristics is proposed. To achieve quadruple band-notched characteristics, two symmetrical branches are added to the ground planes, and three SCRs are etched on the circular patch. The results of the measurements present that the flexible antenna has a frequency range of 2.7–10 GHz. The measured notched frequencies of the antenna are located at 3.1–4 GHz, 4.7–5.5 GHz, 5.7–6.2 GHz, and 7–7.8 GHz. This effectively suppresses interference from WiMAX, WLAN, and X-band satellite communication. All measurement and simulation results demonstrate that the proposed flexible antenna performs well in terms of radiation, within the working frequency range. Furthermore, the antenna exhibits robustness and flexibility when being subjected to bending conditions. With its good interference suppression capabilities and high flexibility, the proposed antenna holds potential applications for wearable applications.

REFERENCES

[1] Ali, T., B. K. Subhash, and R. C. Biradar, "A miniaturized decagonal Sierpinski UWB fractal antenna," *Progress In Electromagnetics Research C*, Vol. 84, 161–174, 2018.

[2] Kumar, O. P., T. Ali, P. Kumar, P. Kumar, and J. Anguera, "An elliptical-shaped dual-band UWB notch antenna for wireless applications," *Applied Sciences*, Vol. 13, No. 3, 1310, 2023.

[3] Arora, S., S. Sharma, R. Anand, and G. Shrivastva, "Miniaturized pentagon-shaped planar monopole antenna for ultra-wideband applications," *Progress In Electromagnetics Research C*, Vol. 133, 195–208, 2023.

[4] Babu, S. R. and P. G. Dinesha, "Design and development of a miniaturized highly isolated UWB-MIMO diversity antenna

with quad band notch characteristics," *Progress In Electromagnetics Research C*, Vol. 131, 197–208, 2023.

[5] Babu, S. R. and P. G. Dinesha, "Design and development of sextuple band reject UWB-MIMO antenna for wireless applications," *Progress In Electromagnetics Research C*, Vol. 128, 231–246, 2023.

[6] Sultan, K. S. and H. H. Abdullah, "Planar UWB MIMO-diversity antenna with dual notch characteristics," *Progress In Electromagnetics Research C*, Vol. 93, 119–129, 2019.

[7] Alazemi, A. J. and Y. T. Alsaleh, "An ultrawideband antenna with two independently tunable notch bands," *Alexandria Engineering Journal*, Vol. 79, 402–410, 2023.

[8] Kumar, P., M. P. MM, P. Kumar, T. Ali, M. G. N. Alsath, and V. Suresh, "Characteristics mode analysis-inspired compact UWB antenna with WLAN and X-band notch features for wireless applications," *Journal of Sensor and Actuator Networks*, Vol. 12, No. 3, 37, 2023.

[9] Iqbal, A., A. Smida, N. K. Mallat, M. T. Islam, and S. Kim, "A compact UWB antenna with independently controllable notch bands," *Sensors*, Vol. 19, No. 6, 1411, 2019.

[10] Premalatha, B., M. V. S. Prasad, and M. B. R. Murthy, "Multiband notched antennas for UWB applications," *Radioelectronics and Communications Systems*, Vol. 62, 609–618, 2019.

[11] Roy, A., A. K. Biswas, A. Nandi, and B. Basu, "Ultra-wideband flexible wearable antenna with notch characteristics for WLAN applications," *Progress In Electromagnetics Research C*, Vol. 129, 143–155, 2023.

[12] Lakrit, S., S. Das, S. Ghosh, and B. T. P. Madhav, "Compact UWB flexible elliptical CPW-fed antenna with triple notch bands for wireless communications," *International Journal of RF and Microwave Computer-Aided Engineering*, Vol. 30, No. 7, e22201, 2020.

[13] Du, C.-Z., Z.-P. Yang, H.-Y. Liu, and Y. Nie, "Four-element CPW-fed UWB MIMO slot antenna with high isolation and triple band-notched characteristics," *Progress In Electromagnetics Research C*, Vol. 116, 145–156, 2021.

[14] You, X., C. Du, and Z.-P. Yang, "A flexible CPW 2-port dual notched-band UWB-MIMO antenna for wearable IoT applications," *Progress In Electromagnetics Research C*, Vol. 128, 155–168, 2023.

[15] Ali, E. M., W. A. Awan, M. S. Alzaidi, A. Alzahrani, D. H. Elkamchouchi, F. Falcone, and S. S. M. Ghoneim, "A shorted stub loaded UWB flexible antenna for small IoT devices," *Sensors*, Vol. 23, No. 2, 748, 2023.

[16] Yassin, M. E., K. F. A. Hussein, Q. H. Abbasi, M. A. Imran, and S. A. Mohassieb, "Flexible antenna with circular/linear polarization for wideband biomedical wireless communication," *Sensors*, Vol. 23, No. 12, 5608, 2023.

[17] Zhao, Z., C. Zhang, Z. Lu, H. Chu, S. Chen, M. Liu, and G. Li, "A miniaturized wearable antenna with five band-notched characteristics for medical applications," *IEEE Antennas and Wireless Propagation Letters*, Vol. 22, No. 6, 1246–1250, 2023.